<u>**Supporting information**</u>

Selective reduction of graphite oxide: A novel approach

Ritwik Panigrahi and Suneel K. Srivastava*.

Department of Chemistry, Indian Institute of Technology, Kharagpur-721302, India.
Email ID: sunil111954@yahoo.co.uk.

Supporting information S1

Materials

Graphite Micro-850 was received as gift from The Asbury Graphite Mills, INC, Asbury, Warren County, NJ. Sodium nitrate was supplied from S. D. Fine Chemicals, India. Potassium permanganate, hydrogen peroxide, hydrazine hydrate, Fehling's solution and concentrated sulfuric acid were obtained from Merck, India. Metallic sodium was purchased from Sisco Research Laboratory, Mumbai, India. Methanol, Ethanol and acetone were procured from SRL Pvt., Mumbai, India.

Preparation of SGO

0.1 g of earlier prepared GO was dispersed in 50 ml of methanol in a 100 cc round bottom flask fitted with a condenser. Following this, one drop of conc. H_2SO_4 was added to it and heated under stirring condition at 95^0C for 10 hours. After that, ~5 g of metallic sodium was added into it and again heated for 24 hours. Finally, the resultant product (SGO) was centrifuged and dried in vacuum for 24 hours.
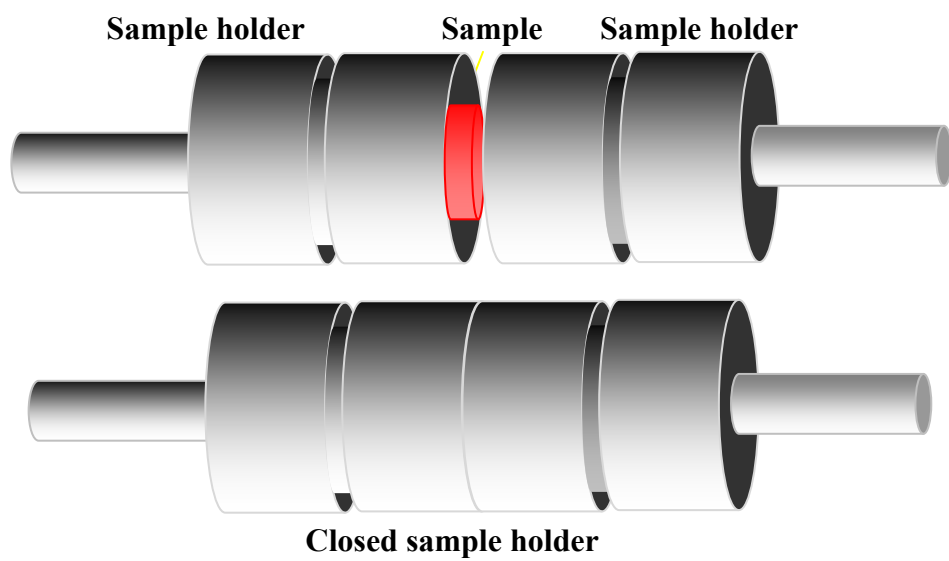
Preparation of RSGO, RSGOCu2, RSGOCu5, RSGOCu10, RGOCu10

0.5 g of SGO was dispersed in 10 ml Fehling's solution (5 ml Fehling's A+ 5 ml Fehling's B + 50ml H_2O) through ultra-sonication, followed by heating under continuous stirring at 90 ^oC for about 8 hours. Subsequently, 5 ml hydrazine monohydrate was added slowly into it and stirred for 24 hours under identical conditions. The product so formed (RSGOCu10) was centrifuged several times with dilute HCl as well as deionized water to

remove excess hydrazine monohydrate and left for vacuum drying at room temperature for 36 hours. The same procedure was followed by using 5 ml Fehling's reagent (2.5 ml Fehling's A+2.5 ml Fehling's B+55 ml H_2O) for RSGOCu5 and 2 ml Fehling's reagent (1 ml Fehling's A+1 ml Fehling's B+58 ml H_2O) to prepare SRGOCu2 samples. Similar experiment were also conducted by using 0.5 g GO and 10 ml Fehling's reagent (5 ml Fehling's A+ 5 ml Fehling's B) to prepare RGOCu10.

Supporting information S2

Instruments.

X-ray diffraction (XRD) analysis was carried out at room temperature on a Phillip, Holland instrument with CuKα radiation (0.1541 nm) in the scanning range of 20° to 75°, scanning rate of 5° per min. FTIR analysis was recorded with a Perkin-Elmer FTIR Spectrometer RXI using KBr discs and thin films over the wave number range 400–4000 cm^{-1}. X-ray photoelectron spectroscopy (XPS) was performed on a PHI 5000 Versa Probe II (ULVAC–PHI, INC, Japan) system using a microfocused (100 lm, 25 W, 15 kV) monochromatic Al Ka source (hm = 1,486.6 eV), a hemispherical analyzer, and a multichannel detector. The typical vacuum in the analysis chamber during the measurements was in the range of 1 9 10–10 Torr. Charge neutralization was used for all measurements using a combination of low

energy Ar^+ ions and electrons. The binding energy scale was charge referenced to the C 1s at 284.6 eV. Elemental compositions were determined from the spectra acquired at pass energy of 117.4 eV. The morphological analysis has been done by field emission scanning electron microscopy (FESEM) on a Carl Zeiss at an accelerating voltage of 20 kV respectively. Transmission electron micrographs was performed on TECNAI G^2, SEI (Netherland) instrument operating at 200kV was used to obtain digitally acquired images on a Gatan multipole charge-coupled device (CCD) camera for the samples placed on carbon-coated Cu grid from dispersion in ethanol. The conductivity measurement was done by a four-probe digital multimeter (Scientific Equipment Roorkee, Model-LCS-02) at room temperature using the powdered compressed pellets. EMI shielding performance of the samples was explored using ENA Series Network Analyzer, E5071C, Agilent Technology. The S_{11} and S_{12} parameter measurements were carried out in the both S-band and X-band frequency of ISM band with a wave guide of diameter 2 cm. Therefore, the circular compressed pellets of the samples having 1cm diameter and 0.5 mm thickness were prepared and placed between wave guide flanges of network analyzer.

Schematic diagram of internal block diagram related to methodology adopted in
EMI shielding experiment.

Supporting information S3

X-ray diffraction (XRD) patterns of GO, SGO, RSGOCu2, RSGOCu5, RSGOCu10, Cu and RSGO are displayed in **Figure S3**. GO showed the presence of an intense peak at $2\theta=10^{o}$ due to (001) plane[1] When GO is selectively reduced by Na/CH$_3$OH, this peak completely disappeared. A new hump is set in at around $2\theta= 24^{o}$ (002) in SGO, which is similar to reduced graphite oxide prepared using normal reducing agents, e.g. NaBH$_4$, N$_2$H$_4$, hydroquinone, thermal treatments etc.[2]This could be ascribed to the expulsion of oxygen-containing functional groups from GO to form reduced graphite oxide (SGO). It is also noted that XRD pattern of SGO remained unaltered on its further reduction with N$_2$H$_4$ (RSGO) .When Fehling's solution is added to the dispersion of SGO and in-situ reduced by N$_2$H$_4$ to form RSGOCu2, RSGOCu5 and RSGOCu10, a hump like peak of RSGO including three peaks corresponding to Cu appeared in XRD.
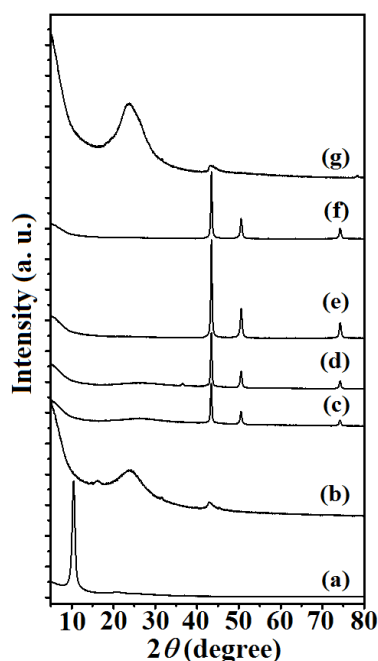
Figure S3 XRD patterns of (a) GO, (b) SGO, (c) RSGOCu2, (d) RSGOCu5, (e) RSGOCu10, (f) Cu nanoparticles, (g) RSGO.

Supporting S4

Figure 2 show deconvoluted FTIR spectra of FSGO2, FSGO5, FSGO10, FSGO15, FSGO20 and FGO10 (F: Fehling's solution, S: selectively reduced, GO: graphite oxide, 2,5,10,15,20 refer to the total volume of 1:1 Fehling solution A and B) prepared by adding Fehling's solution to SGO according to **Table T1**. The presence of peaks at ~3500 and ~3200 cm^{-1} corresponds to OH stretching and H bonded OH bonds stretching between OH of SGO and/COO^{-} in Fehling's reagent. Further, full width half maximum (FWHM) values of peaks corresponding to ~3200 cm^{-1} has been used to calculate approximate (%) of H-bonding in FSGO and FGO according to **Table ST1**.. It is noted that the values in FSGO2, FSGO5, FSGO10, FSGO15, FSGO20 and FGO10 values are found to be 73, 79,83,72,75 and 20 respectively. M These findings clearly show that % H-bonding is always significantly higher in all SGO dispersed Fehling solution. However, the values decreased in FSGO15 and FSGO20 in all probability due to saturation of Fehling molecules. Interestingly, ~20% O-H groups in FGO10 participates in H-bonding compared to all FSGO samples due to unavailability of sufficient O-H groups. Alternatively, the possibility of satiric crowding created between -COOH group of GO and bulky *bistartrato* group of Fehling's solution also cannot be ruled out.

In summary, these studies established that SGO is capable of forming more interaction (H-bonding) compared to GO with Fehling's solution. Though, Fehling's solution has been selected in our work as an interacting complex, other complexes capable of forming H-bond may also be investigated following our novel selective reduction approach.

Table ST1 % H-bonding (approximate) from the FWHM values obtained from the FTIR deconvulation curves for FSGO and FGO samples.

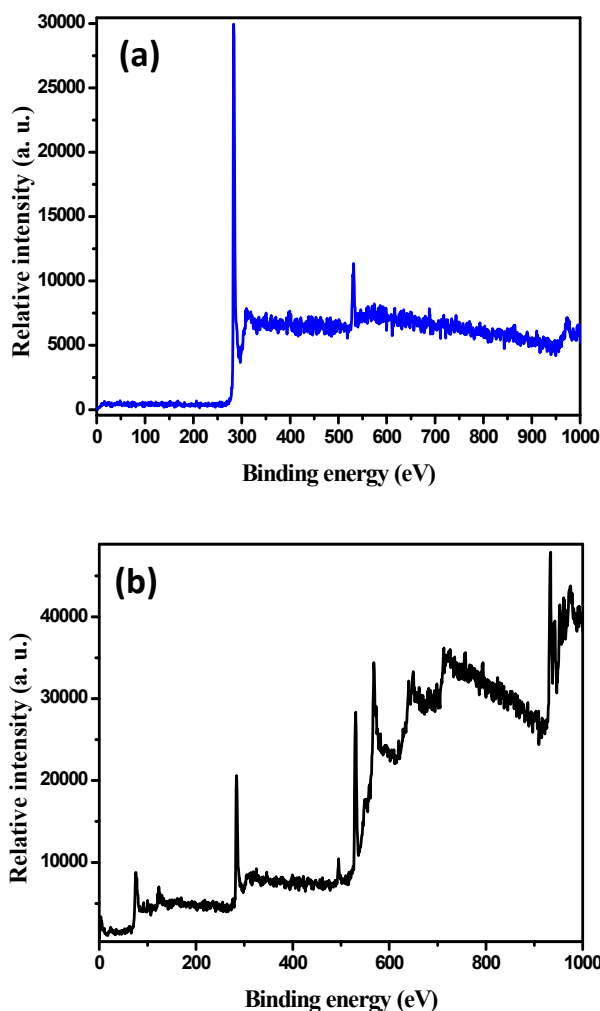| Sample	FWHM (~3200 cm^{-1})	FWHM (~3500^{-1})	~H-bonding (%)
FSGO2	672	244	72
FSGO5	1034	274	79
FSGO10	542	109	84
FSGO15	507	191	73
FSGO20	902	293	74
FGO10	298	1024	20

Figure S5 XPS analyses of (a) RSGO, (b) RSGOCu10

XPS analyses of RSGO and RSGOCu10 samples are displayed in Figure S5. It is noted that the intensity of peak (284.6 eV) appears due to C1s and another small peak at 531.45 eV corresponding to O1s due to the presence of oxygenated functional groups.[3] In case of RSGOCu10, the peak appeared at 284, 933, 953 and 962 eV indicating the formation of elemental copper.[4] Interestingly, XPS data also showed shifting of $\approx$1 eV of O1s (530.32 eV) peak with respect to RSGO (531.45 eV) indicating significant interaction between RSGO and Cu.

Supporting information S6
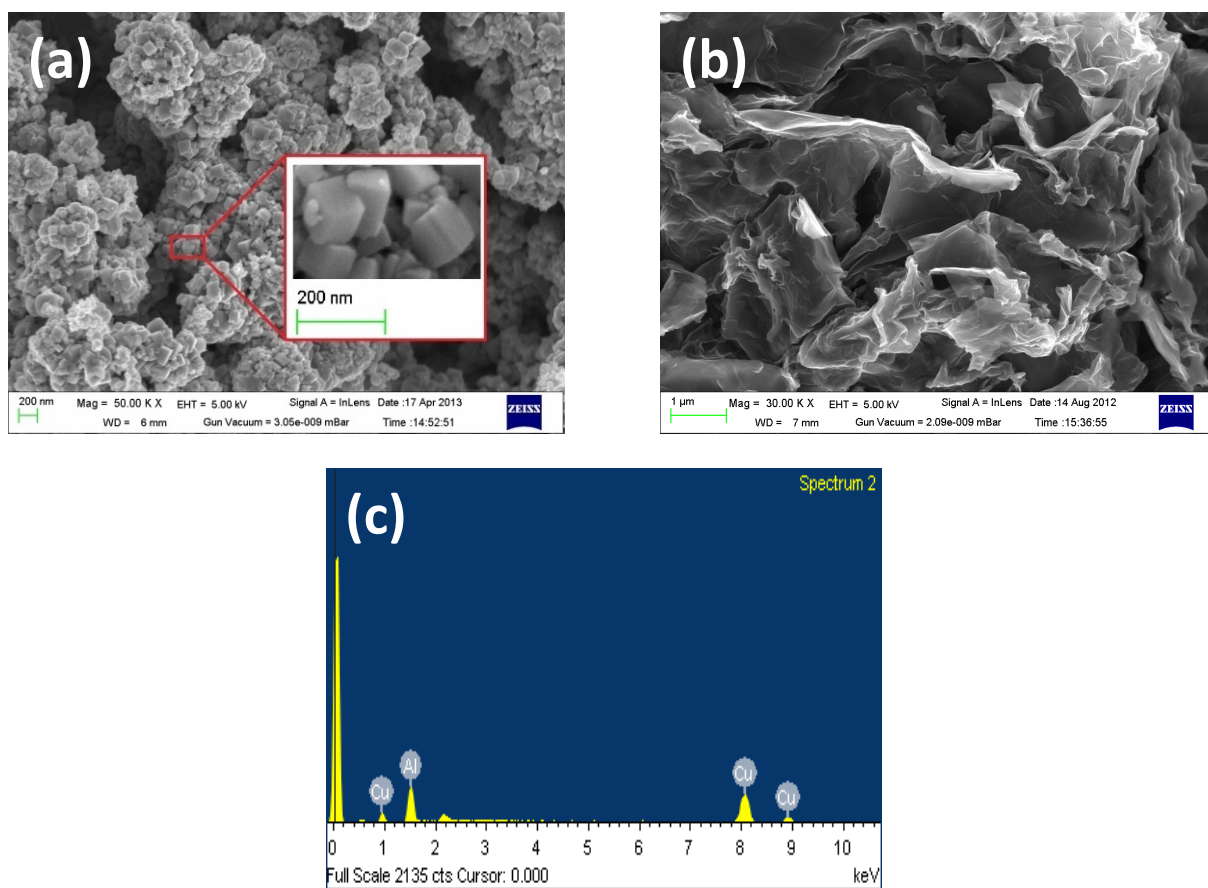
Figure S6 SEM images of (a) Cu nanoparticles, (b) RSGO, (c) EDAX analysis of RSGOCu10.

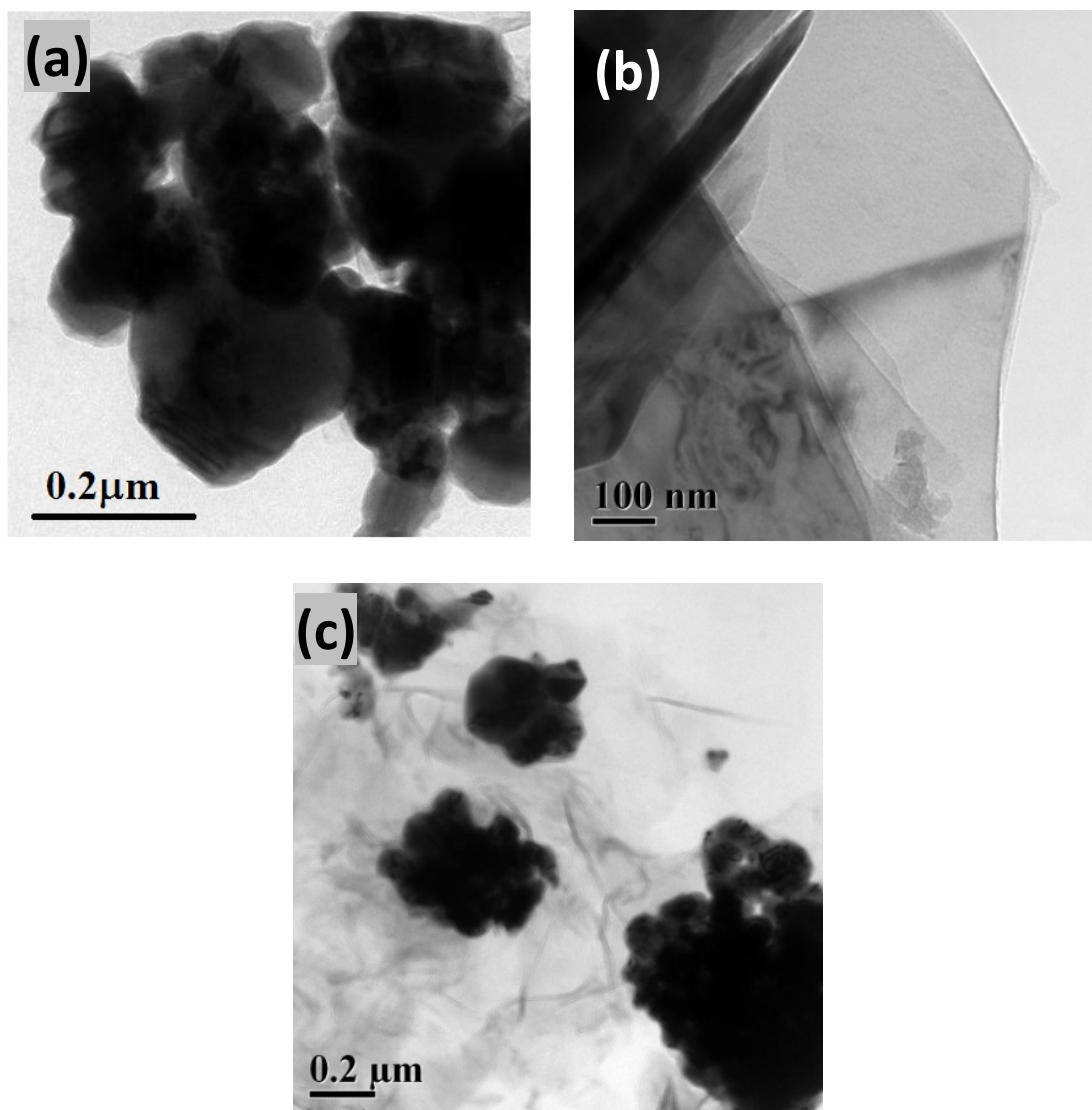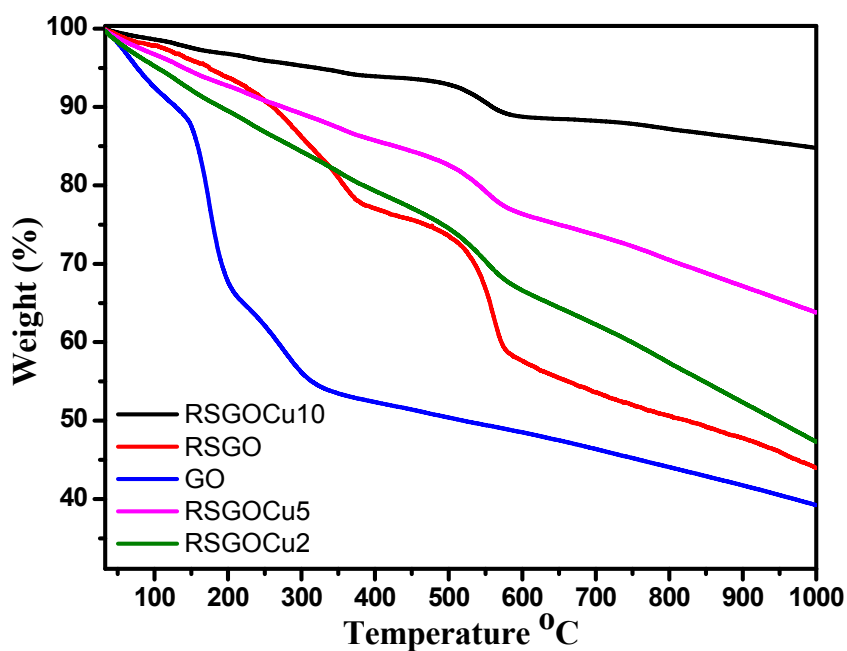**Supporting information S7**

**Figure S7** TEM images of (a) Cu nanoparticles, (b) RSGO, (c) RGOCu10

Supporting information S8

Figure S8 shows TGA of GO, RSGO and RSGOCu10 in the temperature range of 30-1000 ^{0}C under N_2 atmosphere. It is observed that GO exhibits ~13-15% weight loss at around 200 ˚C due to evaporation of absorbed water in GO. It is followed by second 40-45% weight loss in the range of 200-450 ^{0}C due to degradation and expulsion of oxygen containing functional groups present in GO.[5] In contrast, weight loss in first and second steps in RSGO/copper nanocomposites (RSGOCu2, RSGOCu5, and RSGOCu10) are associated with relatively lower weight loss ~7-10 and 8-20 % due the absorbed residual water compared to GO (48%) and RSGO. This observation clearly suggests that the labile oxygen containing groups of GO are reduced during hydrazine hydrate reduction.[6]

Figure S8 TGA of GO, RSGO, RSGOCu2, RSGOCu5, RSGOCu10
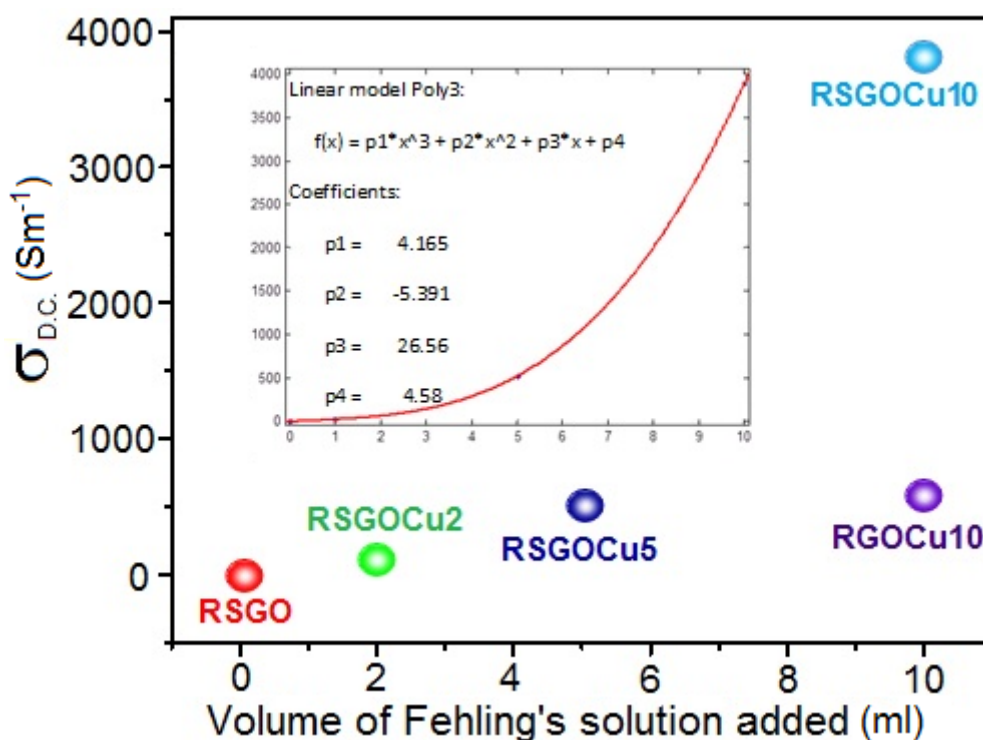
Figure S9 Room temperature D. C. conductivity of RSGO, RSGOCu2, RSGOCu5, RSGOCu10 and RGOCu10. Value of D. C conductivity has been plotted as a function of volume of Fehling's solution added. (Inset Polynomial fitting curve of the points corresponding to RSGO, RSGOCu2, RSGOCu5 and RSGOCu10 using "Matlab" software. The corresponding function and the coefficients of the polynomial are given in the inset. The conductivity value for RGOCu10 is not included in the polynomial curve fitting. Details explanation is given in the main manuscript.)

Supporting information S10

Development of wireless technology in the fields of communication and data transport device manifestations has received considerable worldwide attention in last few years. However, this leads an additional worldwide problem associated with the electromagnetic interference of the various electromagnetic signals generated by these instruments.[7] As a consequence, speed and perfection of signal transport originating from any source is weakened or disrupted. This results in loss of energy, time, data storage and human health. In order to generate and transport the microwave wave signals without any interference, instrument needs to be isolated/shield from the undesirable external radiations from the surroundings. Therefore, several light weight materials have been developed for broadband absorption and shielding purposes.[8-14] All these investigations established reflection to be one of the key parameter in shielding of radiations. The shielding involved electromagnetic field interaction of incoming external radiation with the movable charges (electrons, holes) of a material. As a result, Ag,[15] Fe,[16] Ni,[17]Au,[18] Ag, Au,[19] Fe alloys,[20] Fe oxides, CuO[21] has been widely used in shielding of electromagnetic radiations. However, performance of magnetic Fe, Co, Ni, Fe (and their alloys) are restricted due to environmental corrosion, areal oxidation aging and short life span in many practical applications.[15,16] Additionally, the high cost of noble metals (Ag and Au) restricted their applications as shielding materials. This motivated us to alternatively explore other cheaper materials for effective EMI shielding. In this perceptive, copper (Cu) could be one of the most appropriate choice due to its relatively low cost, high conductivity and its environmental stability. However, it suffers from its heavy weight, film processing difficulties including environmental aging due to corrosion.[17] Therefore, it would be interesting to develop the composites of Cu with other suitable light weight, hydrophobic and environmentally stable materials. In this regard, different forms of carbon, such as graphite[18,19] and its exotic forms[20,21,8] like carbon black[22] expanded graphite[23] as well as reduced graphite oxide,[24] and graphene,[25]carbon fibres,[26,27] single (SWNTs) or multiwall carbon nanotubes (MWNTs)[28] could play an important role. In view of this, we selected Fehling solution as a source of copper (Cu) metal as well as COO⁻ and experienced better dispersion of Cu nanoparticles

on the RSGO sheet formed by in-situ reduction of SGO and Fehling's solution compared to that achieved by simple GO under identical conditions.

When electromagnetic radiation interacts with any material, reflection (SE_R), absorption (SE_A), multiple internal reflections (SE_M) account for partial shielding, where as remaining fraction is transmitted through it. The total shielding efficiency, SE_T (dB) is related to SE_R, SE_A and SE_M as SE_T (dB) = $SE_R + SE_A + SE_M$. It may be noted that the contribution of SE_M is negligible corresponding to SE_T value 12-15 dB. Therefore, above equation is transformed as

$$SE_T (dB) \sim SE_R + SE_A$$

Mathematically SE_T (dB) can be expressed as:

$$SE_T (dB) = 10 \log_{10} (P_T/P_I) = 20 \log_{10} (E_T/E_I) = \log_{10} (H_T/20H_I)$$

Where P_I / E_I and P_T / E_T are the power of incident and transmitted electric field intensity respectively. The absorptivity (A), reflectivity (R) and transmissivity (T) coefficients can be expressed in terms of scattering parameters (S_{11} / S_{22} and S_{12} / S_{21}),

$$T = (E_T/E_I)^2 = |S_{12}|^2 = |S_{21}|^2$$

$$R = (E_R/E_I)^2 = |S_{11}|^2 = |S_{22}|^2$$

These are helpful in calculating A on the basis of R and T as below.[29,30]

$$A = (1- R- T)$$

The complex permittivity ($\varepsilon* = \varepsilon' - i\varepsilon''$) has been calculated using the scattering parameters (S_{11} and S_{21}) obtained from VNA instrument followed by applying standard Nicholson–Ross and Weir theoretical calculations[12]

The total shielding efficiency, SE_T (dB) is related to SE_R, SE_A and SE_M as

$$SE_T (dB) = SE_R + SE_A + SE_M$$

In contrary, the dissipation of electrical energy can be explained through the complex part (ε'') of the electromagnetic parameters.[15] It may be mentioned that the real part of permittivity is related as $\varepsilon' = C/C_o = Q/Q_o = (Q_o + Q')/Q_o$ where Q', C, Q (and C_o, Q_o) correspond to induced charge, specific capacitance, electric charge of materials under experiment (and in vacuum) respectively. When reverse electric field is applied, Q' is decreased leading to the corresponding retardation of electronic oscillation at high frequency.[31] **Figure S10(A)** shows variation of reflection with frequency (2-8GHz) of RSGO, RGOCu10, RSGOCu2, RSGOCu5 and RSGOCu10 which is elaborately discussed in the main manuscript. The frequency variation of both ε' and ε'' also corroborated this inference in our case. Though, value of ε' of RSGO (ε' ~41-5) is very close to RSGOCu1 (ε''~44-20) in the frequency range 2-8 GHz as evident from **Figure S10(B)**, the corresponding values in RSGOCu5 and RSGOCu10 lies in the range of 215-46 and 187-61 respectively. **Figure S10 (C)** show that ε'' of RSGO (10-1) and RSGOCu1 (15-8) closer over the entire frequency range. Interestingly, significantly higher values of 108-19, 77-27 is observed in RSGOCu5, RSGOCu10 respectively. All these observations could be explained on the basis of conductivity of both Cu as well as RSGO. In all probability, higher conductivity of the corresponding composites due to presence of highly conducting Cu in RSGO in corresponding nanocomposites could account for the observed increased values of ε' and ε''. Our observation are also found to be relevant to previous work on Ag nanoparticles loaded polyaniline/graphene composites.[32] This could also be attributed to dipolar and electrical polarization in a material induced by its polarizability in presence of microwave. The polarizability again is influenced by the permittivity which depends on conductivity and electric polarization of a material. So for that reason it can be said that with increasing conductivity the values of ε' and ε'' increases. Interestingly it is observed that in case of RGOCu10 the values of ε' and ε'' are in the range 25-14 and 7-4.5 respectively. Though the values are higher than RSGO but very lower compared to RSGOCu10, even if lower than the corresponding lowest Cu loaded composite RSGOCu2. This observation also supports that as conductivity of RGOCu10 is lower compared to RSGOCu10, its ε' and ε'' also follow the same trend.

Figure S10(D) shows the frequency dependent plot of dielectric tangent loss factor (tan δ_E) of RSGO, RSGOCu2, RSGOCu5, RSGOCu10 and RGOCu10 in the frequency range 2-8 GHz. It is observed that dielectric tangent loss is in the range 0.24-0.19 in RSGO. In case of RGOCu10, the value is nearly close to 0.3 over the entire range. Interestingly, tanδ_E value in RSGOCu2, RSGOCu5 and RSGOCu10 are found to be significantly higher and lie in the range of 0.38-0.35, 0.5-0.42 and 0.4-0.44 respectively. This inference has been elaborately discussed in the main manuscript.[15]
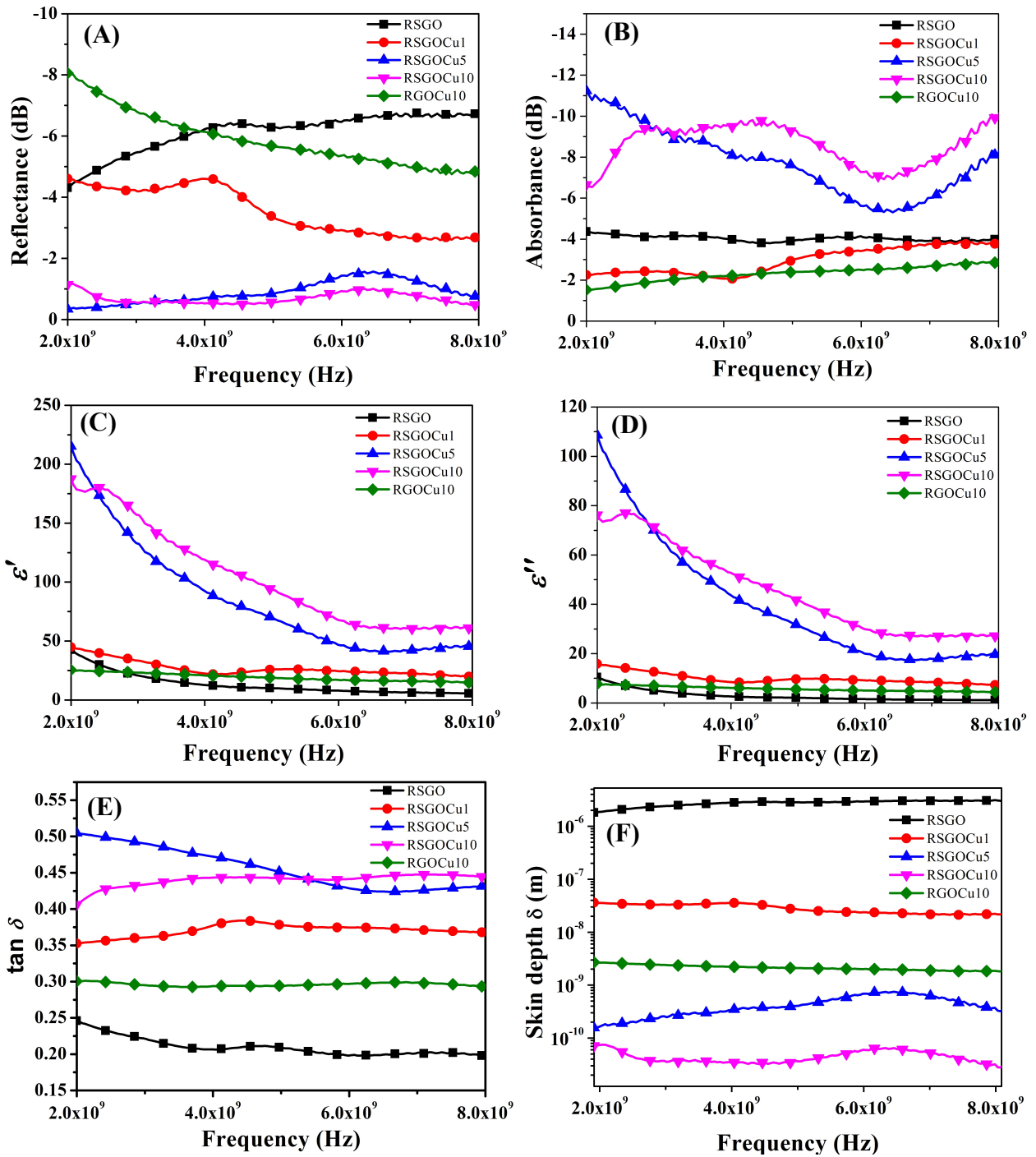
Figure S10 (A) Variation of reflection loss, (B) absorption loss, (C) real part (ε') of the room temperature complex permittivity **(D)** imaginary part (ε'') of the room temperature complex permittivity and **(E)** room temperature tangent loss and (F) skin depth (δ) versus frequency (2-8 GHz) of RSGO, RSGOCu2, RSGOCu5, RSGOCu10 and RGOCu10.
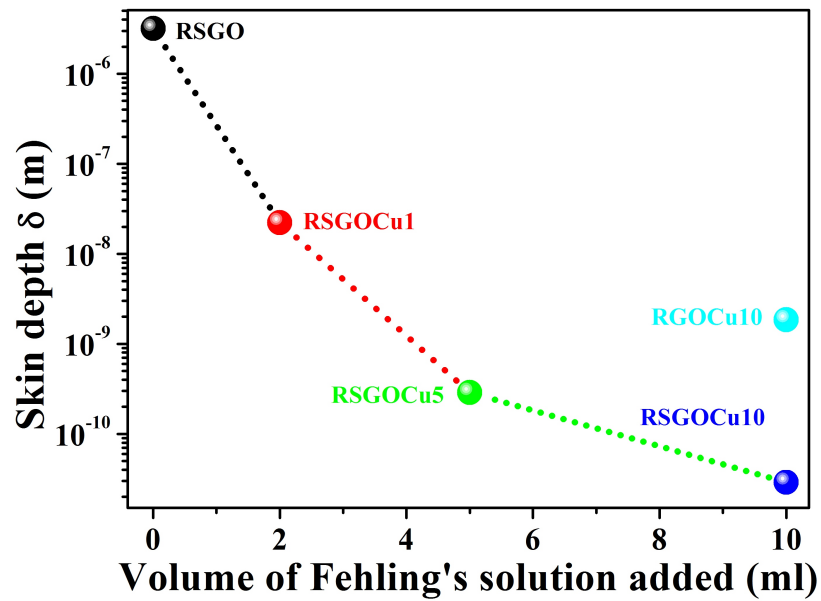
Figure S11 Skin depth values of RSGO, RSGOCu2, RSGOCu5, RSGOCu10 and RGOCu10 has been plotted as a function of volume of Fehling's solution added.

Table ST2

No	materials	Thickness	Frequency	EMI shielding (dB)	Ref.
1	Ni-P-Cu plated polyether ether ketone/carbon fiber composites (CFs/PEEK)		30 to 1,500 MHz	76 dB	33
2	carbon–copper (C–Cu) nanocomposites	2 mm	12-18 GHz	58.7 dB	34
3	MWNT/PS CNW/PS	240 μm	X band	~37 dB ~13 dB	35
4	polyaniline-coated graphite oxide/g-Fe2O3/BaTiO3		1000-3000	~37	36
5	Graphene	1mm	8-12 GHz	~38	37

	oxide/ferrofluid/cement composites				
6	Graphene film MWNTs film	0.15	8-12 GHz	35.8 41.0	38
7	Cu–Ni alloy integrated with graphene	1.5 mm 1 mm 0.5 mm	8-12	Average 33 Maximum peak 42dB 28 dB 22 dB	39
8	8.7 vol % filled Ni powder in PISO 9.4 vol % filled Ni powder in PES	2.95mm 2.8 mm	2 GHz 2 GHz	44 dB 25.5 dB	40
9	20 vol% Nickel fibres PES composites	3.17 mm	2	13.2	40
10	9.4 vol %Ni particles PES-matrix composites	30-56 μm	2	23	41
11	19 vol %Ni fiber PES-matrix composites	1 mm	2	5	42
12	7 vol %Ni fiber PES-matrix composites	2 mm	2	58	42
13	7 vol %Ni filaments PES-matrix composites	100 μm	2	87	42.
14	RGO/Fe3O4/Ag	2.6mm	9.0 GHz	58.1 dB	43

References

(1) C.Xu, X. D.Wu, J. W. Zhu, X. Wang, *Carbon,* 2008, *46*, 386–389.

(2) (a) M. H.-Alonso, A. A. Abdada, M. J. McAllister, I. A. Aksay, R. K. Prud'- homme, *Langmuir,* 2007, *23*, 10644–10649. (b) T. Szabo, O. Berkesi, P. Forgo, K. Josepovits, Y. Sanakis, D. Petridis, I. Dekany, *Chem. Mater*. 2006, *18*, 2740–2749.

(3) (a) Q. Chen, H. Huang, W. Chen, A. T. S. Wee, Y. P. Feng, J. W. Chai, Z. Zhang, J. S. Pan, S. Wang, *J. Appl. Phys. Lett*. 2010, *96*, 072111−072113. (b) T. Seyller, K. Emtsev, F. Speck, K. Gao, L. Ley, *Appl. Phys. Lett*. 2006, *88*, 242103−242105.

(4) N. Cioffi, L. Torsi, N. Ditaranto, G. Tantillo, L. Ghibelli, L. Sabbatini, T. Bleve-Zacheo, M. D'Alessio, P. G. Zambonin, E. Traversa, *Chem. Mater.* 2005, *17*, 5255-5262.

(5) Z. Fang , A. Ito, A. C. Stuart, H. Luo, Z. Chen, K. Vinodgopal, W. You, T. J. Meyer, D. K. Taylor,.*Langmuir*, 2013, **7**,7992.

(6) D.Wang, G. Ye, X. Wang, *Adv. Mater.* 2011**, *23***, 1122.

(7) Y. Yang, M. C. Gupta, K. L. Dudley, R. W. Lawrence, *Nanoletters* 2005, *5*, 2131.

(8) A. P. Singh, M. Mishra, P. Sambyal, B. K. Gupta, B. P. Singh, A. Chandra, and S. K. Dhawan, *J. Mater. Chem. A*, 2014, *2*, 3581

(9) P. Saini, V. Choudhary, B. P. Singh, R. B. Mathur, S. K. Dhawan, *Mater. Chem. Phys*. 2009, *113*, 919.

(10) R. C. Che, L. M. Peng, X. F. Duan, Q. Chen, X. L. Liang, *Adv. Mater*. 2004, *16*, 401.

(11) J. M. Thomassin, X. D. Lou, C. Pagnoulle, A. Saib, L. Bednarz, I. Huynen, R. Jérôme, C. Detrembleur, *J. Phys. Chem. C* 2007, *111*, 11186.

(12) Z. G. An, S. L. Pan, J. J. Zhang, *J. Phys. Chem. C* 2009, *113*, 2715.

(13) P. Xu, X. J. Han, J. J. Jiang, X. H. Wang, X. D. Li, A. H. Wen, *J. Phys. Chem. C* 2007, *111*, 12603.

(14) P. Saini, V. Choudhary, B. P. Singh, R. B. Mathur, S. K. Dhawan, *Synth. Met.* 2011, *161*, 1522.

(15) P. Saini, V. Choudhary, N. Vijayan, and R. K. Kotnala, *J. Phys. Chem. C* 2012, *116*, 13403−13412.

(16) X. Shui, D. D. L. Chung, *J. Electron. Mater*. 1995, *24*, 107.

(17) Y. Ma, E. Lombi, I. W. Oliver, A. L. Nolan, and M. J. Mclaughlin, *Environ. Sci. Technol.* 2006, *40*, 6310-6317.

(18) G. Tong, W. Wu, Q. Hua, Y. Miao, J. Guan, and H. Qian, *J. Alloys Compd*., 2011, *509*, 451–456.

(19) T. GuoXiu, Y.JinHao, M. Ji, Q. M. Yue, G. J. Guo, L. L. Chao, G. PeiJun and C. JianJing, *Sci. Sin. Chim.,* 2011, *41*, 1121− 1126.

(20) D. D. L. Chung, *Carbon*, 2001, *39*, 279–285.

(21) A. P. Singh, M. Mishra, A. Chandra, and S. K. Dhawan, *Nanotechnology*, 2011, *22*, 9.

(22) N. C. Das, D. Khastgir, T. K. Chaki, and A. Chakraborty, *Composites, Part A*, 2000, *31*, 1069–1081.

(23) M. Mishra, A. P. Singh, and S. K. Dhawan, *J. Alloys Compd.,* 2013, *557*, 244–251.

(24) A. P. Singh, P. Garg, F. Alam, K. Singh, R. B. Mathur, R. P. Tandon, A. Chandra, and S. K. Dhawan, *Carbon*, 2012, *50*, 3868–3875.

(25) A. P. Singh, M. Mishra, A. Chandra, and S. K. Dhawan, *Nanotechnology*, 2011, *22*, 9.

(26) S. Yang, K. Lozano, A. Lomeli, H. D. Foltz, and R. Jones, *Composites, Part A*, 2005, *36*, 691–697.

(27) L. Li, and D. D. L. Chung, *Composites*, 1994, *25*, 215–224.

(28) A. P. Singh, B. K. Gupta, M. Mishra, Govind, A. Chandra, R. B. Mathur and S. K. Dhawan, *Carbon*, 2013, *56*, 86–96.

(29) N. Li, Y. Huang, F. Du, X. He, X. Lin, H. Gao, Y. Ma, F. Li, Y. S. Chen, P. C. Eklund, *Nano Lett*. 2006, *6*, 1141−1145.

(30) J. Wang, C.Xiang, Liu, Q. Pan, Y. Guo, *J. Adv. Funct. Mater.* 2008, *18*, 2995−3002.

(31) C. Wang, Xj Han, P. Xu, XL Zhang, Yc Du, S. R. Hu, *Appl. Phys. Lett*. 2011, *98*, 072906.

(32) Y. Chen, Y. Li, M. Yip, N. Tai, *Composite Science and Technology*, 2013**, *80***, 80-86.

(33) Y. Su, B. Zhou, L. Liu, J. Lian, G. Li, *Polymer Compos*. 2014 DOI 10.1002/pc

(34) A. Kumar, A. P. Singh, S. Kumari, P. K. Dutta, S. K. Dhawana, A. Dhar, *J. Mater. Chem. A*, 2014, *2*, 16632

(35) J. Chau, G. A. Gelves, C. Bellehumeur, U. Sundararaj, **ANTEC**

(36) Y. E. Moon, J. Yun, H. Kim, *J. Industrial and Engineering Chem.*,2013, *19*, 493–497

(37) A. P. Singh, M. Mishra, A. Chandra, S. K. Dhawan, *Nanotechnology*, 2011, *22,* 465701 (9pp)

(38) V. Eswaraiah *,* V. Sankaranarayanan *,* A. K. Mishra *,* S. Ramaprabhu *,*2010 *International Conference on Chemistry and Chemical Engineering* (ICCCE 2010)

(39) K. Ji, H. Zhao, Z. Huang, Z. Dai, *Materials Letters,* 2014, **122**, 244–247

(40) L. Li, D. D. L. Chung, *Polymer compos.*, 1993, **6**, 14

 (41) D.D.L. Chung, *Carbon,* 2001, **39**, 279–285

(42) X. Shui, D D L. Chung, *J Electron Mater,* 1997, **26(8)**, 928–34.

 (43) M. Zong, Y. Huangn, H. Wu, Y. Zhao, S. Wang, N. Zhang, W. Zhang, *Materials Letters,* 2013, **111**, 188–191